X-ray spectroscopy reveals high symmetry and electronic shell structure of transition-metal-doped silicon clusters

J. T. Lau,* K. Hirsch, Ph. Klar, A. Langenberg, F. Lofink, R. Richter, J. Rittmann, M. Vogel, V. Zamudio-Bayer, and T. Möller
Institut für Optik und Atomare Physik, Technische Universität Berlin, EW 3-1, Hardenbergstraße 36, D-10623 Berlin, Germany

B. v. Issendorff
Fakultät für Physik, Universität Freiburg, Stefan-Meier-Straße 19, D-79104 Freiburg, Germany
(Received 22 January 2009; published 22 May 2009)

Size-selected cationic transition-metal-doped silicon clusters have been studied with x-ray absorption spectroscopy at the transition-metal $L_{2,3}$ edges to investigate the local electronic structure of the dopant atoms. For VSi_{16}^+, the x-ray absorption spectrum is dominated by sharp transitions which directly reveal the formation of a highly symmetric silicon cage around the vanadium atom. In spite of their different number of valence electrons, a nearly identical local electronic structure is found for the dopant atoms in $TiSi_{16}^+$, VSi_{16}^+, and $CrSi_{16}^+$. This indicates strongly interlinked electronic and geometric properties: while the transition-metal atom imposes a geometric rearrangement on the silicon cluster, the interaction with the highly symmetric silicon cage determines the local electronic structure of the transition-metal dopant.

DOI: 10.1103/PhysRevA.79.053201 PACS number(s): 36.40.Cg, 61.46.Bc, 73.22.−f

I. INTRODUCTION

Doped silicon clusters are perfect examples of tailoring nanoparticle properties by choice of size and composition. Since silicon prefers sp^3 bonding or even higher coordinated bonds reminiscent of its high pressure metallic phases [1], pure silicon clusters tend to form complex and rather compact structures [2–5], but never form cages as carbon does. Incorporation of a single impurity atom, however, rearranges the geometric and electronic structure of small silicon clusters completely. In particular, this can lead to a stabilization of the otherwise unfavorable cage structures [6–9]. Prominent examples are $ScSi_{16}^-$, $TiSi_{16}$, and VSi_{16}^+, which are highly stable and therefore largely abundant in mass spectra [10–14] because of simultaneous electronic and geometric shell closure [8,9]. Their electronic stability is reflected in a large highest occupied molecular orbital–lowest unoccupied molecular orbital gap of about 2 eV, which has been predicted theoretically [6–9] and was confirmed by photoelectron spectroscopy for the case of $TiSi_{16}$ [14]. The formation of silicon cages can be inferred experimentally from reactivity [14–18], photodissociation [19], and physisorption [20] studies. Indirect evidence is supplied by photoelectron spectroscopy [12,14,16,17,21–24].

Despite a wealth of theoretical and experimental work, the electronic structure and nature of bonding in these silicon cages is still controversial [6–9,12,14,17,24]. Two competing models are commonly used, rationalizing the electronic structure obtained from *ab initio* calculations [7,8] either on the basis of the empirical 18 (in this case rather 20) electron rule [8,25,26] known for transition-metal compounds in chemistry or on electronic shell closure of delocalized electrons in a spherical potential model combined with an approximate selection rule for the angular momentum [7,9,27,28]. In a simplified description, the first model explains stability on the grounds of electronic shell closure at the transition-metal atom, while the second model considers electronic shell closure in the spherical potential of the entire cluster cage.

II. EXPERIMENTAL SETUP

We have used x-ray absorption spectroscopy on size-selected free clusters [29] as a local and element-specific probe to clarify the local electronic structure of the dopant atom that leads to the exceptional stability of doped silicon cages. Transition-metal-doped silicon cluster cations are produced in a magnetron sputtering source by co-sputtering of two targets. After size selection in a quadrupole mass selector, clusters are stored in a liquid nitrogen cooled linear Paul trap. Along the trap axis, electronic transitions are excited by a collinear beam of tunable soft x-ray radiation. Ions are subsequently extracted from the trap and are analyzed in a time-of-flight mass spectrometer. X-ray absorption spectra are obtained in ion yield mode by monitoring the yield of cluster fragment ions as a function of incident photon energy.

III. RESULTS

Vanadium $L_{2,3}$ x-ray absorption spectra of free, size-selected VSi_n^+ clusters with $n=14-18$ are presented in Fig. 1. In this size range, VSi_{16}^+ is a prominent line in mass spectra [12,14]. Compared to other clusters, the x-ray absorption spectrum of VSi_{16}^+ exhibits the best resolved structure with sharp lines, which directly indicate a high degeneracy of electronic levels and a high symmetry of this cluster. Adding or removing silicon cage atoms lowers the symmetry and broadens electronic transitions as in VSi_{17}^+ or VSi_{15}^+. The origin of the distinct double peak structure observed for VSi_{16}^+ in resonant excitation at the $L_3(2p_{3/2}\rightarrow 3d,4s)$ and $L_2(2p_{1/2}\rightarrow 3d,4s)$ edges will be discussed below.

*tobias.lau@physik.tu-berlin.de

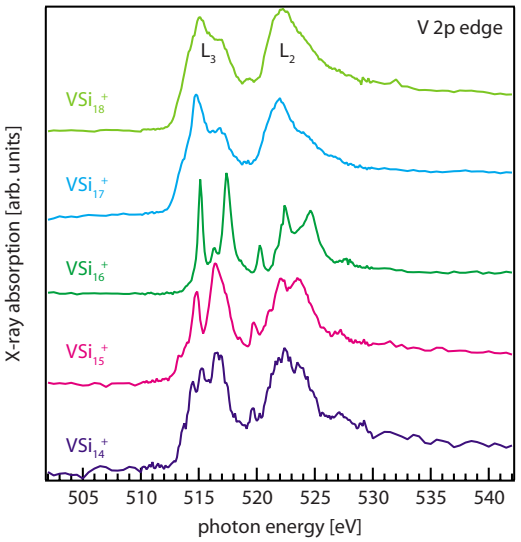

FIG. 1. (Color online) $L_{2,3}$ x-ray absorption spectra of size-selected VSi_n^+ clusters ($n=14-18$). The VSi_{16}^+ spectrum is characterized by the sharpest lines, indicating a highly symmetric cage with high degeneracy of the electronic levels. The double peak structure can be linked to the electronic density of states in tetrahedral symmetry.

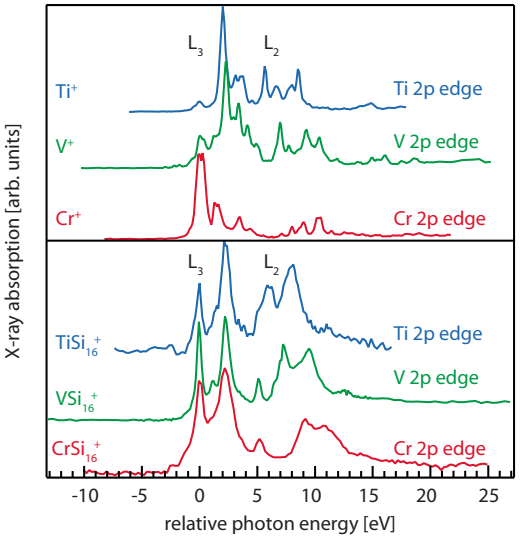

FIG. 2. (Color online) Transition-metal $L_{2,3}$ x-ray absorption spectra of $TiSi_{16}^+$, VSi_{16}^+, and $CrSi_{16}^+$ cage clusters in the lower panel, and of bare Ti^+, V^+, and Cr^+ ions [29] in the upper panel. The spectra are aligned at the first peak position. While bare ions show differing spectra, the relative excitation energy in doped silicon clusters is nearly identical. This surprising fact indicates almost identical local electronic structure at the dopant atom site. Relative positions of the L_2 edge shift because of decreasing $2p$ spin-orbit splitting from chromium to titanium. In the titanium spectrum, the 5 eV feature of the L_3 line is partially masked by overlapping L_2 intensity.

When keeping the number of silicon atoms constant but changing the dopant atom from vanadium to titanium or chromium, the number of valence electrons in the cluster is changed by ± 1. The resulting x-ray absorption spectra of $TiSi_{16}^+$, VSi_{16}^+, and $CrSi_{16}^+$ are shown in the lower panel of Fig. 2. For ease of comparison, the spectra are aligned at the first peak position of the transition-metal L_3 excitation and are given on a relative photon energy scale. Surprisingly, titanium, vanadium, and chromium exhibit a very similar fine structure in their x-ray absorption spectra when embedded in Si_{16} cages; the relative excitation energies are practically identical for all three dopant atoms. Not only the intense lines at 0 and 2.1 eV, but also the less intense features at 1.1 and 5.0 eV are reproduced in all spectra. This indicates a nearly identical local electronic density of states at the transition-metal atoms and a very similar geometry of their environment, as x-ray absorption spectroscopy is very sensitive to both [30]. For comparison, the spectra of the bare transition-metal ions are displayed in the upper panel of Fig. 2. As expected, the multiplet structure is characteristic for each element and reflects the differences in electronic structure, namely, the different $3d$ orbital occupancies. Apparently, these differences disappear when the atoms are located in Si_{16} cages. Here, titanium and chromium adopt the same local electronic structure as vanadium in VSi_{16}^+ in spite of their differing number of valence electrons. Obviously, the interaction with the highly symmetric silicon cage determines the electronic structure of the dopant.

X-ray absorption spectroscopy was also performed at the silicon $L_{2,3}$ edges. As representative examples, the spectra of Si_{16}^+ and VSi_{16}^+ are compared in Fig. 3. While pure silicon clusters in this size range generally show broad spectra similar to the one of Si_{16}^+, the spectrum of VSi_{16}^+ shows sharp lines, which indicate a well structured electronic density of states that reflects the high symmetry of the cluster. Although x-ray absorption is not a direct probe of the ground-state electronic structure, and there is no simple one-to-one correspondence of the x-ray absorption spectra to the unoccupied density of states, this again hints at highly degenerate electronic states.

IV. DISCUSSION

These findings can be well understood within the spherical potential model [7,9,28,31], which was originally devel-

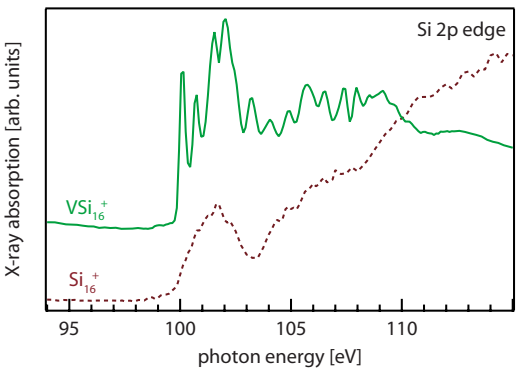

FIG. 3. (Color online) Silicon $L_{2,3}$ x-ray absorption spectra of Si_{16}^+ (dashed line) and VSi_{16}^+ (solid line) clusters. The high symmetry of doped silicon cage clusters is again reflected in the highly structured x-ray absorption spectrum, with sharp transitions as compared to pure silicon clusters. $TiSi_{16}^+$ and $CrSi_{16}^+$ show features similar to VSi_{16}^+.

oped to explain the nature of bonding in pure and endohedral fullerenes [27,28,31–33]. A transition-metal-doped Si_{16} Frank-Kasper polyhedron [6,34] possesses a total of 64 (i.e., 16×4) silicon valence electrons; additional valence electrons are supplied by the transition-metal atom hosted at the center of the cage. Because of the nearly spherical shape of the cluster, its valence orbitals can be classified by an angular momentum quantum number l and a radial quantum number n in harmonic oscillator notation. In a simplified view, one can regard bonding within the spherical Si_{16} shell to be mediated by "σ" orbitals $(1s,1p,1d,1f,1g)$ without radial nodes [31,35,36], while bonding to the transition-metal dopant is promoted by "π" orbitals $(2s,2p,2d)$ with one radial node [31,35,36]. These orbitals hybridize with transition-metal valence orbitals of the same angular momentum quantum number according to the approximate l-selection rule [27,28]. In particular, the transition-metal $4s$ and $3d$ orbitals hybridize with silicon cage s and d "π" orbitals to form bonding $(2s,2d)$ and antibonding $(3s,3d)$ orbitals. In fact more than these four levels are formed: as the Frank-Kasper Si_{16} cage [6,34] is not perfectly spherically symmetric but has tetrahedral (T_d) symmetry, a d state is represented as $(e+t_2)$. Therefore the metal $3d$ orbitals can interact with all silicon cage orbitals having e or t_2 components and do so especially with the energetically close-by $1h$ $(e+t_1+2t_2)$ states. This leads to the formation of three groups of electronic states with major contributions of metal $3d$ orbitals [9].

The resulting schematic density of states of VSi_{16}^+ [7,9] is shown in Fig. 4: a total of 68 (i.e., $16\times4+5-1$) valence electrons occupy all states of the σ $(n=1)$ system up to the $1g$ level and of the π $(n=2)$ system up to the $2d$ level, which forms the highest occupied molecular orbital of the cluster. The lowest unoccupied molecular orbital has $1h$ character [9] and there is a large $2d-1h$ gap [6–9]. As discussed above, the metal atom $3d$ orbitals contribute to the completely filled cage $2d$ orbital as well as to two narrow groups of unoccupied levels above the gap, which are about 2 eV apart. Since the vanadium $2p$ core hole is created locally at the dopant site in the x-ray absorption process, and dipole transitions are allowed from the vanadium $2p$ core level into unoccupied local orbitals with d or s angular momentum character, these sharp features of the electron density of states show up in the x-ray absorption spectrum of VSi_{16}^+ and can explain the double structure of the L_3 and L_2 lines for this closed shell species.

The similarity of the titanium and chromium spectra can be understood in the same picture: in the case of "nonmagic" open shell $TiSi_{16}^+$ and $CrSi_{16}^+$ cage clusters with 67 (i.e., $16\times4+4-1$) and 69 (i.e., $16\times4+6-1$) valence electrons, respectively, the energetic ordering of the orbitals should remain very similar, as the nearly identical spectra in Fig. 2 demonstrate that the silicon cage retains its highly symmetric structure. In $CrSi_{16}^+$, the additional valence electron is then accommodated in the $1h$ orbital above the $2d-1h$ gap. Because of the dominant silicon contribution to this $1h$ orbital [9], the electron can be expected to reside mainly at the silicon cage. The local unoccupied $4s$ and $3d$ electronic states of the dopant, which are probed by chromium $L_{2,3}$ x-ray absorption spectroscopy, are therefore hardly affected

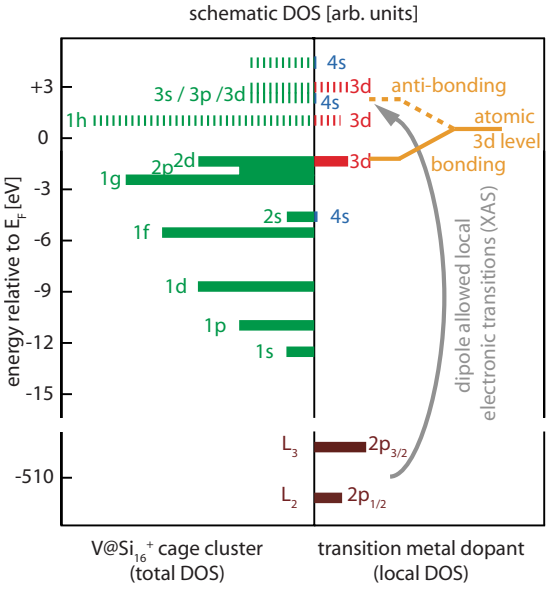

FIG. 4. (Color online) Schematic view of the VSi_{16}^+ density of states (DOS). The total DOS is shown in the left panel while the local l-projected DOS at the dopant site [9] is shown in the right panel. In x-ray absorption spectroscopy at the spin-orbit split transition-metal $2p$ levels, electronic transitions are allowed only into *local*, *d*- or *s*-projected states. Therefore, only states marked with an arrow $(3d,4s)$ are probed. The splitting of the metal $3d$ states into bonding and antibonding states is indicated schematically.

by this additional valence electron, for which reason the $CrSi_{16}^+$ and VSi_{16}^+ x-ray absorption spectra are nearly identical in their main features. The slight broadening observed for $CrSi_{16}^+$ is probably due to Jahn-Teller deformation because of the open electronic shell situation [37].

Similarly, in the case of $TiSi_{16}^+$ with its 67 valence electrons, the electron missing to the closed electronic shell leads to a $2d^9$ configuration of the cluster. Since the cluster $2d$ orbital has most of its weight at the Si_{16} cage [9], only a fraction of the hole is located at the titanium dopant. Again, the small change in the local $3d$ occupancy of the transition-metal dopant has a negligible influence on the x-ray absorption spectrum. In the three cases of $TiSi_{16}^+$, VSi_{16}^+, and $CrSi_{16}^+$ considered here, the interaction with the electronic structure of the highly symmetric silicon cage results in a nearly identical local electronic structure of the dopant and leads to the very similar x-ray absorption spectra observed experimentally. In this respect, x-ray absorption spectroscopy is complementary to valence band photoelectron studies, because the former gives insight into the *local* electronic structure while the latter probes *global* properties.

In principle the explanation given above is very close to the crystal-field splitting model usually applied to explain the x-ray absorption spectra of transition-metal ions in compounds [30]. In VSi_{16}^+, the vanadium ion occupies a tetrahedral site at the center of the Si_{16} cage. This cage is tetravalent because of the four electrons missing to the $2d$ electron shell closing. The vanadium ion contributes its four valence electrons to bonding orbitals leaving no $3d$ electrons in localized antibonding states. Formally this leads to a local $3d^0$ con-

figuration at the vanadium site. This empty $3d$ orbital is split into e and t_2 states because of the tetrahedral symmetry of its environment [38], which causes the double peak structure of the x-ray absorption spectrum [30]. Obviously, the same formal $3d^0$ configuration is adopted by the chromium and titanium ions as well. In all three cases the electronic shell structure of the cage causes a formal transfer of the $3d$ valence electrons from the metal atoms to the silicon cage, and the cage symmetry determines the structure of the x-ray absorption spectra.

Finally, the "magic" behavior of the closed electronic shell cluster VSi_{16}^+ [12,14] can be related to spherical aromaticity [36]: including the vanadium atom valence electrons in the electron count, the Si_{16}^{4-} cage has 18 electrons in π ($n=2$) states and 50 electrons in σ ($n=1$) states. Consequently, both π and σ states follow the $2(N+1)^2$ rule of spherical aromaticity [36], with $N=4(1g)$ for σ states and $N=2(2d)$ for π states. Indeed, based on nucleus independent chemical shifts [39], cage aromaticity, predicted recently for Si_{16}^{4-} cages, has been proposed to explain the stability of $TiSi_{16}$ clusters [24,40] and can now be traced back to closed electronic shells.

V. SUMMARY

To summarize, x-ray absorption spectroscopy reveals nearly identical local electronic states of the dopant atoms in $TiSi_{16}^+$, VSi_{16}^+, and $CrSi_{16}^+$, showing how closely electronic and geometric properties are interlinked in highly symmetric doped silicon clusters. This demonstrates that x-ray absorption spectroscopy of size-selected gas phase clusters is a very powerful technique which can contribute to the understanding of electronic structure and bonding in isolated nanoparticles. Because of its element-specific nature, this technique is particularly useful for the study of mixed systems and is very promising in view of doped metal clusters, clusters-adsorbate complexes, or molecules in well defined solvation shells.

ACKNOWLEDGMENTS

We would like to thank L. C. Balbás, M. B. Torres, and E. M. Fernández for discussions of the electronic density of states. All data were taken at the Berlin synchrotron radiation facility BESSY II beamline U49/2-PGM-1. Technical assistance by BESSY II staff members Gerd Reichardt and Olaf Schwarzkopf is gratefully acknowledged. Travel to BESSY was supported by BMBF. This project was partially funded by TUB as research initiative project under Grant No. FIP 2/60 and by Deutsche Forschungsgemeinschaft SFB 508. J.R. acknowledges financial support by Villigst-Stiftung.

[1] S. Minomura and H. G. Drickamer, J. Phys. Chem. Solids **23**, 451 (1962).
[2] M. F. Jarrold and E. C. Honea, J. Phys. Chem. **95**, 9181 (1991).
[3] K.-M. Ho, A. A. Shvartsburg, B. Pan, Z.-Y. Lu, C.-Z. Wang, J. G. Wacker, J. L. Fye, and M. F. Jarrold, Nature (London) **392**, 582 (1998).
[4] K. A. Jackson, M. Horoi, I. Chaudhuri, T. Frauenheim, and A. A. Shvartsburg, Phys. Rev. Lett. **93**, 013401 (2004).
[5] J. Bai, L.-F. Cui, J. Wang, S. Yoo, X. Li, J. Jellinek, C. Koehler, T. Frauenheim, L.-S. Wang, and X. Zeng, J. Phys. Chem. A **110**, 908 (2006).
[6] V. Kumar and Y. Kawazoe, Phys. Rev. Lett. **87**, 045503 (2001).
[7] V. Kumar, Comput. Mater. Sci. **36**, 1 (2006).
[8] J. Ulises Reveles and S. N. Khanna, Phys. Rev. B **74**, 035435 (2006).
[9] M. B. Torres, E. M. Fernández, and L. C. Balbás, Phys. Rev. B **75**, 205425 (2007).
[10] S. M. Beck, J. Chem. Phys. **87**, 4233 (1987).
[11] S. M. Beck, J. Chem. Phys. **90**, 6306 (1989).
[12] K. Koyasu, M. Akutsu, M. Mitsui, and A. Nakajima, J. Am. Chem. Soc. **127**, 4998 (2005).
[13] S. Neukermans, X. Wang, N. Veldeman, E. Janssens, R. Silverans, and P. Lievens, Int. J. Mass Spectrom. **252**, 145 (2006).
[14] K. Koyasu, J. Atobe, M. Akutsu, M. Mitsui, and A. Nakajima, J. Phys. Chem. A **111**, 42 (2007).
[15] H. Hiura, T. Miyazaki, and T. Kanayama, Phys. Rev. Lett. **86**, 1733 (2001).
[16] M. Ohara, K. Miyajima, A. Pramann, A. Nakajima, and K. Kaya, J. Phys. Chem. A **106**, 3702 (2002).
[17] M. Ohara, K. Koyasu, A. Nakajima, and K. Kaya, Chem. Phys. Lett. **371**, 490 (2003).
[18] A. Negishi, N. Kariya, K. Sugawara, I. Arai, H. Hiura, and T. Kanayama, Chem. Phys. Lett. **388**, 463 (2004).
[19] J. B. Jaeger, T. D. Jaeger, and M. A. Duncan, J. Phys. Chem. A **110**, 9310 (2006).
[20] E. Janssens, P. Gruene, G. Meijer, L. Wöste, P. Lievens, and A. Fielicke, Phys. Rev. Lett. **99**, 063401 (2007).
[21] W. Zheng, J. M. Nilles, D. Radisic, and J. Kit H. Bowen, J. Chem. Phys. **122**, 071101 (2005).
[22] A. Grubisic, H. Wang, Y. J. Ko, and K. H. Bowen, J. Chem. Phys. **129**, 054302 (2008).
[23] K. Koyasu, J. Atobe, S. Furuse, and A. Nakajima, J. Chem. Phys. **129**, 214301 (2008).
[24] S. Furuse, K. Koyasu, J. Atobe, and A. Nakajima, J. Chem. Phys. **129**, 064311 (2008).
[25] S. N. Khanna, B. K. Rao, and P. Jena, Phys. Rev. Lett. **89**, 016803 (2002).
[26] J. Ulises Reveles and S. N. Khanna, Phys. Rev. B **72**, 165413 (2005).
[27] K. Jackson, E. Kaxiras, and M. R. Pederson, J. Phys. Chem. **98**, 7805 (1994).
[28] K. Jackson and B. Nellermoe, Chem. Phys. Lett. **254**, 249 (1996).
[29] J. T. Lau, J. Rittmann, V. Zamudio-Bayer, M. Vogel, K. Hirsch, P. Klar, F. Lofink, T. Möller, and B. v. Issendorff, Phys. Rev.

Lett. **101**, 153401 (2008).
[30] F. M. F. de Groot, J. Electron Spectrosc. Relat. Phenom. **67**, 529 (1994).
[31] C. Yannouleas and U. Landman, Chem. Phys. Lett. **217**, 175 (1994).
[32] H. W. Kroto, Nature (London) **329**, 529 (1987).
[33] T. Guo, M. D. Diener, Y. Chai, M. J. Alford, R. E. Haufler, S. M. McClure, T. Ohno, J. H. Weaver, G. E. Scuseria, and R. E. Smalley, Science **257**, 1661 (1992).
[34] F. C. Frank and J. S. Kasper, Acta Crystallogr. **11**, 184 (1958).
[35] J. L. Martins, N. Troullier, and J. H. Weaver, Chem. Phys. Lett. **180**, 457 (1991).
[36] A. Hirsch, Z. Chen, and H. Jiao, Angew. Chem. Int. Ed. **39**, 3915 (2000).
[37] H. A. Jahn and E. Teller, Proc. R. Soc. Lond. A Math. Phys. Sci. **161**, 220 (1937).
[38] F. Beeler, O. K. Andersen, and M. Scheffler, Phys. Rev. B **41**, 1603 (1990).
[39] Z. Chen, C. Wannere, C. Corminboeuf, R. Puchta, and P. von Ragué Schleyer, Chem. Rev. **105**, 3842 (2005).
[40] Z. F. Chen, S. Neukermans, X. Wang, E. Janssens, Z. Zhou, R. E. Silverans, R. B. King, P. von Ragué Schleyer, and P. Lievens, J. Am. Chem. Soc. **128**, 12829 (2006).